JOURNAL OF CATALYSIS 117, 1–18 (1989)

The Reduction Behavior of Silica-Supported and Alumina-Supported Iron Catalysts: A Mössbauer and Infrared Spectroscopic Study

A. F. H. WIELERS,[1] A. J. H. M. KOCK,[2] C. E. C. A. HOP, J. W. GEUS,[3] AND A. M. VAN DER KRAAN

Department of Inorganic Chemistry, University of Utrecht, Croesestraat 77a, 3522 AD Utrecht, The Netherlands, and Interuniversitair Reactor Instituut, Mekelweg 15, 2629 JB Delft, The Netherlands

Received May 16, 1986; revised August 31, 1988

The reduction behavior of Fe/Al_2O_3 and Fe/SiO_2 catalysts is investigated using *in situ* Mössbauer spectroscopy and infrared spectra of adsorbed CO. Controlled injection at constant pH (= 6) of an acidified iron(III)nitrate solution into a suspension of the support leads to the formation of highly dispersed supported α-FeOOH particles (2–8 nm). Reduction of the Fe/Al_2O_3 catalyst is found to proceed via a stabilized $Fe_{1-x}O$ phase according to the sequence α-$FeOOH/Fe_3O_4/Fe_{1-x}O/\alpha$-Fe. Reduction for 15 h at 873 K leads to iron crystallites 20–30 nm in diameter. It is shown that these surfaces still contain traces of oxygen. This is in accordance with single crystal investigations which indicate that the reduction of iron surfaces is a surface-sensitive process: full reduction of small particles (consisting of more open surfaces) is virtually impossible. Moreover, it is established that upon high-temperature evacuation following hydrogen reduction the iron surfaces are severely oxidized by water molecules formed by hydrocondensation of hydroxyl groups from the support. Reduction of the Fe/SiO_2 catalyst proceeds via an iron(II)silicate phase, which at higher temperatures is partly reduced to α-Fe. Small iron particles (10 nm) densely and homogeneously distributed over the support are obtained by prolonged reduction (up to 150 h) at 723 K, whereas severe sintering occurs upon reduction for relatively short periods (16 h) at temperatures above 823 K. With the silica-supported iron catalyst the iron crystallites appear to be (partly) encapsulated by an iron(II)silicate layer. The encapsulation of the silica-supported iron particles, the incomplete reduction of the alumina-supported iron particles, and the reoxidation occurring upon high-temperature evacuation presumably account for the small extent of room temperature hydrogen chemisorption usually found with supported iron catalysts.

INTRODUCTION

As a result of the important industrial applications of iron catalysts a great number of publications have appeared dealing with the characterization of iron surfaces (*1–6*). Investigations focusing on the reduction behavior of iron catalysts have shown that the nature of the catalyst support strongly affects the rate of reduction to metallic iron. There is considerable experimental evidence that intermediate, rather thermostable iron/support compounds develop during the reduction process. Yuen *et al.* (*1*) have suggested that during reduction of a 1 wt% Fe/SiO_2 catalyst ferrous ions are formed strongly interacting with the silica. With Fe/MgO samples the formation of $Fe_xMg_{1-x}O$ has been detected (*2*). Recently, *in situ* magnetic susceptibility measurements have been reported which were collected during the reduction of a 25 wt% Fe/γ-Al_2O_3 catalyst showing that reduction proceeds via a stabilized $Fe_{1-x}O$ phase, according to the sequence α-$Fe_2O_3/Fe_3O_4/Fe_{1-x}O/\alpha$-Fe (*3*). Unexpectedly, also with small iron particles deposited onto a carbon support (carbon is known for its negligible affinity for iron) the presence of an Fe^{2+} species after reduction has been reported (*4*). Niemantsverdriet *et al.* advanced that

[1] Present address: Koninklijk/Shell Laboratorium, Badhuisweg 3, 1031 CM Amsterdam, The Netherlands.

[2] Present address: Nederlandse Philips Bedrijven B.V., P.O. Box 218, 5600 MD Eindhoven, The Netherlands.

[3] To whom all correspondence should be addressed.

0021-9517/89 $3.00

this species is located at the interface between the iron particles and the carbon support (*4*). It cannot be excluded, however, that the Fe^{2+} species are due to submonolayer levels of oxygen still present in the metal–gas interface after reduction.

Depending on the experimental conditions and the nature of the support, different intermediate iron compounds are thus formed during reduction. With the experimental techniques at disposal generally the exact oxidation state of the surface is beyond direct experimental assessment. Knowledge of the surface oxidation state is of great importance with regard to the catalytic properties of supported catalysts. A study that relates the oxidation state of the surface to that of the bulk can provide us with the information needed to understand how the catalytic activity depends on (i) the reduction procedure and on (ii) the nature of the support used. However, such investigations have only rarely been reported.

In this paper results obtained with *in situ* Mössbauer spectroscopy and *in situ* infrared spectroscopy will be reported for Fe/Al_2O_3 and Fe/SiO_2 catalysts of a varying degree of reduction. These techniques are complementary: room temperature Mössbauer spectroscopy can be considered as mainly a bulk characterization technique, whereas infrared spectroscopy gives exclusively information about the surface. Using the infrared spectra of adsorbed carbon monoxide it is thus possible to investigate the surfaces of samples, the bulk oxidation state of which has been determined by means of Mössbauer spectroscopy. Since in both cases thin self-supporting wafers are used, it is ensured that the effect of pretreatment procedures is not affected by differences in the experimental sample geometry making a direct comparison of Mössbauer and infrared experiments legitimate.

With the results a number of purposes will be served. First, the effect of a given reduction procedure and the effect of the support on the ultimate catalytic behavior will be revealed. Second, the effect of evacuation procedures, which generally precede further catalyst characterization, on the surface oxidation state will be evaluated (*5*). Third, the present data will add to resolve the controversy as to whether the activated hydrogen chemisorption on supported iron catalysts is due either to the presence of oxygen in the iron surfaces or to the intrinsic small particle-size effects (*6*).

EXPERIMENTAL

The Fe/Al_2O_3 (25 wt%) and Fe/SiO_2 (20 wt%) catalysts were prepared by slow injection at 293 K of an acidified (pH 1) $Fe(NO_3)_3 \cdot 9H_2O$ solution into a suspension of the support. During the injection the pH was kept constant at 6 by simultaneous injection of a CO_2-free KOH solution. The respective support materials were purchased from Degussa: γ-Al_2O_3 (Degussa-C, 100 m^2/g) and SiO_2 (Aerosil, 200 m^2/g). The presence of δ-Al_2O_3 in the Degussa-C sample cannot be excluded. Full details of this preparation procedure were given in a previous paper (*3*). After filtration and subsequent washing with boiled demineralized water, the catalysts were dried in air at 373 K overnight. Metal loadings refer to dry fully reduced samples.

The procedures and vacuum equipment used in the infrared experiments have been described elsewhere (*7*). Spectra were recorded at room temperature with a Perkin–Elmer 580B infrared spectrophotometer connected to a 3500 CDS data station. Samples were pressed into wafers at a pressure of 80 MPa. In order to increase the rather poor transmittance of the Fe/Al_2O_3 catalyst this sample was diluted with an equal amount of a high surface area alumina (Harshaw AlIII-P, 180 m^2/g). The disks used with the Mössbauer experiments were pressed at 10 MPa. Wafers used in Mössbauer spectroscopy weighed about 200 mg, while those for infrared studies about 30–50 mg. Carbon monoxide (AGA, purity 99.997%) was used in the infrared experi-

ments without further purification. Hydrogen (10 vol% in Ar) of technical quality, used for the reduction in the infrared and Mössbauer experiments, was purified by passing through a "Deoxo catalyst" (BASF R-3-11) and dried over a molecular sieve (Linde 4A).

Mössbauer spectra were recorded with a constant acceleration spectrometer using a ^{57}CO in Rh source (30 mCi). Isomer shifts reported with respect to the NBS standard sodium nitroprusside. Literature isomer shifts, calibrated using a metallic iron foil, have been recalculated and refer to the nitroprusside standard in this paper. Magnetic hyperfine fields were calibrated with the 515 kOe field of α-Fe_2O_3 at room temperature. The spectra were not corrected for the varying distance between the source and the detector and hence the curved background in the measured spectra is of instrumental origin. The Mössbauer parameters were determined by fitting the collected spectra with reference subspectra consisting of Lorentzian-shaped lines using a nonlinear iterative minimization routine. In the case of quadrupole doublets the line widths as well as the absorption areas were constrained to be equal. The Mössbauer spectra were collected at 300, 77, and 4.2 K using a chemical reactor permitting the *in situ* measurement of spectra in any desired gaseous atmosphere (*8*). All reported spectra were measured in a hydrogen atmosphere.

For electron microscopic investigations (Philips EM 420) reduced samples were passivated in air statically, ultrasonically treated in ethanol, and dispersed onto a holey carbon film.

Fischer–Tropsch activity measurements were performed in a continuous-flow system. Details of the experimental setup have been described previously (*9*). The experiments were carried out at atmospheric pressure at a temperature of 553 K, a H_2/CO ratio of 3.0 (partial CO pressure 0.05 bar). Conversions were kept below 3%. The activity is expressed as the rate of conversion of carbon monoxide to hydrocarbons per gram of iron.

RESULTS

Fe/Al_2O_3 Catalyst

The fresh, unreduced, and evacuated (for 0.5 h at 298 K) iron-on-alumina catalyst exhibited no infrared-active adsorption of carbon monoxide.

Figure 1 shows spectra recorded with the Fe/Al_2O_3 catalyst reduced under progressively more severe conditions. After reduction the catalyst was cooled in the hydrogen/argon stream. The catalyst was evacuated at room temperature for half an hour (final pressure about 1×10^{-3} Pa). Next, 13.3 kPa CO was dosed and spectra were recorded. It can be seen that after the first reduction step three bands are present in the spectrum, viz. at 2155, 2050, and 2020 cm^{-1}. After the second reduction step especially the band at 2020 cm^{-1} becomes more pronounced and the peak maximum shifts to a slightly lower wavenumber (2010 cm^{-1}). Upon extending the reduction time at 873 K especially the band at 2050 cm^{-1} intensifies considerably (Fig. 1c). Prolonged exposure (at room temperature) of the reduced catalyst (2 h, 873 K) to the CO

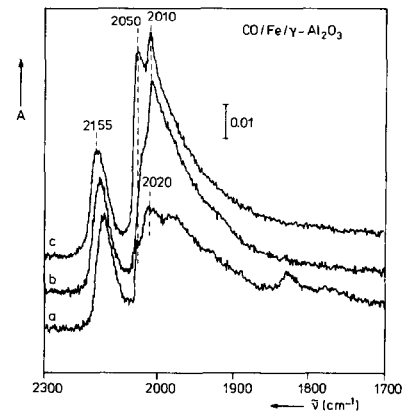

FIG. 1. Infrared spectra of adsorbed CO (13.3 kPa) on Fe/Al_2O_3 catalyst subsequently reduced under increasingly severe conditions: (a) 0.5 h, 773 K; (b) 0.5 h, 873 K; (c) 2 h, 873 K.

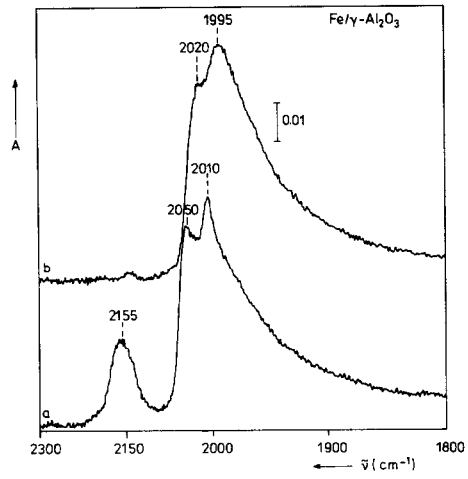

FIG. 2. Infrared spectra of adsorbed CO on Fe/Al_2O_3 catalyst: (a) 13.3 kPa CO dosed after reduction for 15 h at 873 K; (b) after subsequent evacuation at room temperature for 0.5 h.

atmosphere leads to an increase of the intensity of the 2050-cm^{-1} band at the expense of the 2010-cm^{-1} band (not shown). The 2155-cm^{-1} band does not show such a time dependence. We stress that no bands below 2000 cm^{-1} are observed.

Figure 2a shows the spectrum after 15 h reduction at 873 K. Only slight changes are observed compared to the spectrum recorded after reduction for 2 h at 873 K (Fig. 1c). It is shown in Fig. 2b that upon evacuation of the gaseous CO (for 0.5 h at 298 K) the 2155-cm^{-1} band disappears and the band at 2050/2010 cm^{-1} shifts to lower wavenumbers (2020/1995 cm^{-1}). Furthermore, the integrated absorbance of this band increases slightly upon evacuation. A surface coverage dependent extinction coefficient may explain this result. The red shift can be understood as upon evacuation the CO coverage decreases thereby reducing dipole–dipole interactions (*10, 11*).

In order to facilitate the interpretation of the CO infrared features the reduced Fe/Al_2O_3 catalyst was deliberately contaminated with carbon and/or oxygen. With the spectrum recorded in Fig. 3b carbon and oxygen were deposited on the iron catalyst by the following procedure: (i) the reduced catalyst is exposed to 13.3 kPa CO; (ii) gaseous CO is evacuated at room temperature for 0.25 h (only the irreversibly bonded CO remains on the surface (cf. Fig. 2b)); (iii) the catalyst is evacuated at 523 K for 0.30 h; (iv) after cooling down to room temperature a reference spectrum is taken; (v) finally, 13.3 kPa CO is admitted prior to recording the infrared spectrum. By repeating this cycle the amount of carbon and/or oxygen in the surface gradually increases. The reference spectra recorded in step (iv) showed that no molecular CO was present after evacuation at 523 K. The spectrum shown in Fig. 3b is recorded after repeating this cycle three times. It can be seen that the intensity of the 2010-cm^{-1} band strongly decreases in favor of the 2050-cm^{-1} band. Furthermore, a small band appears at 2085 cm^{-1}.

The thus treated Fe/Al_2O_3 catalyst was next exposed to 3.3 kPa CO for 0.5 h at 523 K. With Fe films Körner *et al.* (*12*) have shown that under these conditions iron completely reacts to iron carbide. After evacuation at 523 K the catalyst was cooled to room temperature and 13.3 kPa CO was admitted. From Fig. 3c it appears that although the intensity of the 2050-cm^{-1} band

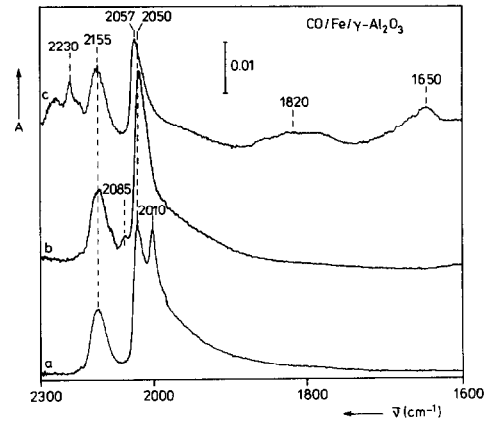

FIG. 3. Infrared spectra of adsorbed CO (13.3 kPa) on (a) clean and (b, c) deliberately contaminated catalyst. Experimental conditions during carbon and/or oxygen contamination are described in the text.

has decreased (the peak maximum is now located at 2057 cm^{-1}), molecular CO adsorption still occurs on such a surface. The 2085-cm^{-1} band has now disappeared from the spectrum, whereas the intensity of the 2155-cm^{-1} band is not affected by the applied treatment. Furthermore, new bands appear at 1650 cm^{-1} (carbonate-like species) (*13*), 1830 and 2230 cm^{-1} (carbon dioxide).

Figure 4 shows the effect of high-temperature evacuation following high-temperature hydrogen reduction. For the spectra in Figs. 4b and 4c the catalyst has not been cooled to room temperature in the hydrogen/argon stream after reduction (15 h, 873 K), but has been evacuated at 823 K for 1.75 and 11 h, respectively. Subsequently, the catalyst was cooled *in vacuo* and next 13.3 kPa CO was admitted. Figure 4b shows that high-temperature evacuation leads to an intensity decrease and a slight shift to lower wavenumbers of the band at 2050/2010 cm^{-1}. The intensity of the 2155 cm^{-1} increases slightly. The 2085-cm^{-1} band again appears in the spectrum. These changes become more pronounced with prolonged evacuation time (Fig. 4c).

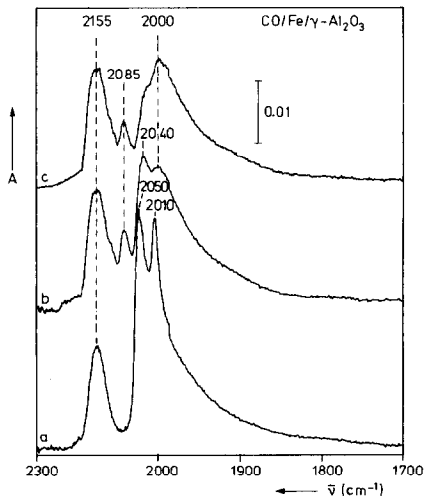

FIG. 4. Infrared spectra of CO illustrating the effect of high-temperature evacuation. Fe/Al_2O_3 catalyst reduced for 15 h at 873 K before subsequent evacuation. Spectra recorded after evacuation: (a) for 0.5 h at 298 K, (b) for 1.75 h at 823 K, and (c) for 11 h at 823 K.

TABLE 1

Mössbauer Parameters of the Spectra Presented in Fig. 5

	T (K)	IS (mm/s)	QS (mm/s)	$\langle H_{eff} \rangle$ (kOe)
Fe/Al_2O_3	300	0.62	0.63	0
	77			
	4.2	0.74		500
Physical mixture of α-FeOOH + Al_2O_3	300	0.62	0.71	0
	77			
	4.2	0.75		500
Fe/SiO_2	300	0.61	0.94	0
	77	0.74	0.96	0
	4.2	0.75		460
α-FeOOH				
Ref. (*16*)	298	0.64		378
	77	0.60		498
Ref. (*27*)	298	0.61		384

Note. IS isomer shift; QS, electric quadrupole splitting; $\langle H_{eff} \rangle$, mean effective hyperfine field.

In separate experiments we established that admission of 11 kPa O_2 for half an hour at room temperature to the (partly) reduced catalyst followed by evacuation and admission of 13.3 kPa CO did not lead to any infrared active adsorption of carbon monoxide. In the spectrum only a weak carbonate-like band was observed (1620 cm^{-1}).

The bulk oxidation state of the Fe/Al_2O_3 sample was determined using Mössbauer spectroscopy. In Fig. 5a the Mössbauer spectra recorded at different temperatures with freshly prepared, unreduced iron-on-alumina catalyst are shown. The room temperature spectrum consists of a doublet with parameters characteristic of a high-spin Fe^{3+} compound. At 77 K the spectrum consists of a superposition of an electric quadrupole doublet and an asymmetrically broadened six-line pattern. At 4.2 K only a magnetically split pattern is observed. The Mössbauer parameters deduced from these spectra are listed in Table 1. They correspond to those of α-FeOOH (goethite). The

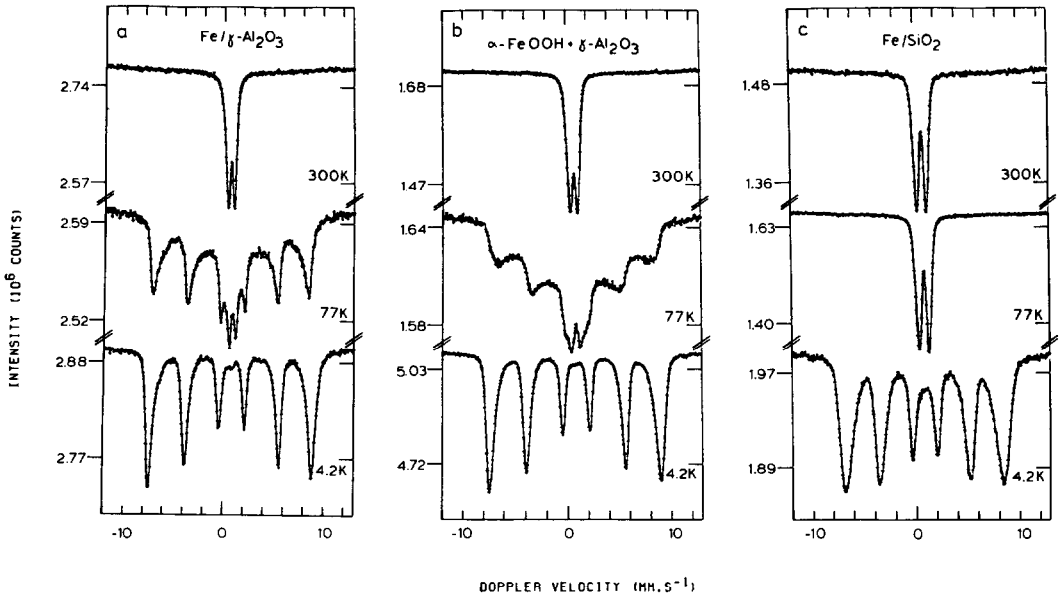

FIG. 5. Mössbauer spectra of freshly prepared samples measured at 300, 77, and 4.2 K.

temperature dependence of the spectra is due to superparamagnetic relaxation allowing an estimation of the dimensions of the α-FeOOH present in the fresh alumina-supported catalyst.

In Fig. 6 the Mössbauer spectra recorded during reduction of the Fe/Al_2O_3 catalyst are shown. After reduction at 573 K for half an hour the Mössbauer spectrum still shows the Fe^{3+} compound. After subsequent reduction at 673 K for 0.5 h characteristic magnetite (Fe_3O_4) lines have appeared, whereas the spectral area due to the Fe^{3+} compound has decreased. After an increasingly severe reduction treatment (773 K, 0.5 h) the intensity of the Fe_3O_4 subspectrum decreases, in favor of a not well-resolved Fe^{2+} doublet (IS = 1.30 mm/s and QS = 0.55 mm/s). Only prolonged high-temperature reduction (873 K, 9h) results in the formation of α-Fe. There is, however, still a significant amount of Fe^{2+} present. It should be pointed out that especially the Fe_3O_4 component shows considerably broadened lines, which points either to the presence of a highly dispersed Fe_3O_4 phase or to the presence of Al ions in the spinel lattice (*14, 15*).

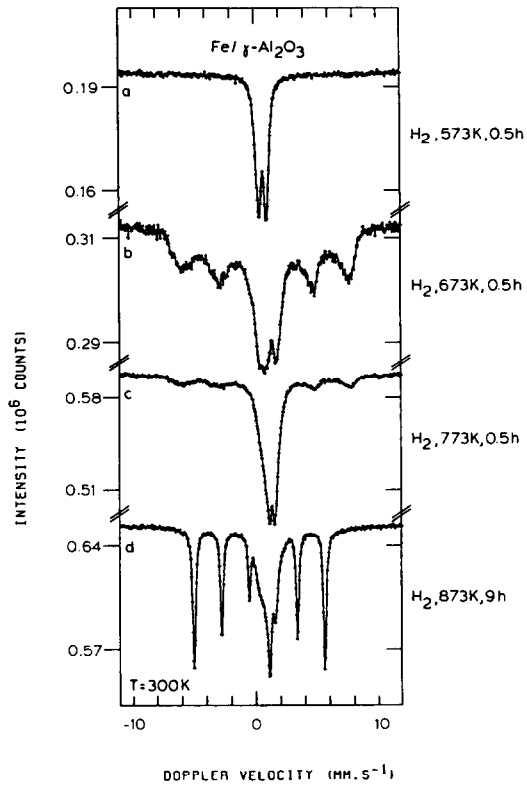

FIG. 6. Room temperature Mössbauer spectra of Fe/Al_2O_3 catalyst subsequently reduced under progressively more severe conditions.

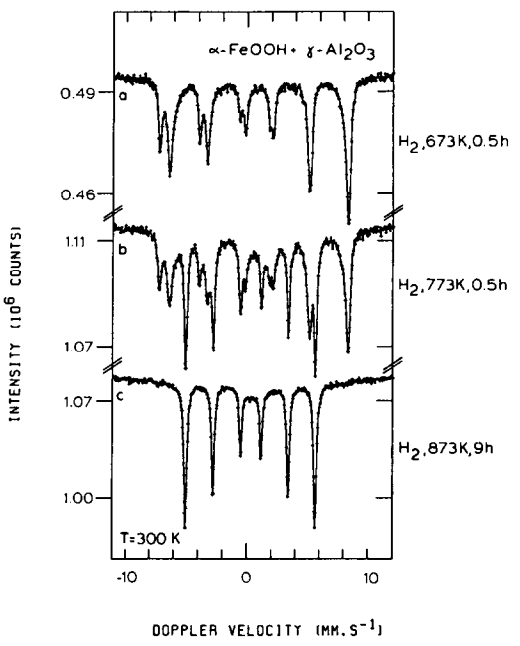

FIG. 7. Room temperature Mössbauer spectra of physical mixture (α-FeOOH and γ-Al_2O_3) subsequently reduced under increasingly severe conditions.

In order to assess the influence of the support on the reduction behavior of supported α-FeOOH the reduction behavior of a physical mixture consisting of α-FeOOH and Al_2O_3 also has been investigated. The unsupported α-FeOOH was prepared analogously to the supported catalyst (*3*). The spectra of the freshly prepared mixture, measured at different temperatures, are shown in Fig. 5b. A comparison of the spectra in Figs. 5a and 5b suggests that the size of the unsupported α-FeOOH particles is slightly smaller than that of the alumina-supported particles. The room temperature Mössbauer spectra collected after reduction under progressively more severe conditions are shown in Fig. 7. The reduction of the physical mixture at 673 K results in the formation of Fe_3O_4, which exhibits Mössbauer parameters (Fe^{3+}, isomer shift, IS = 0.50 mm/s and H_{eff} = 485 kOe; Fe^{2+}, IS = 0.96 mm/s and H_{eff} = 463 kOe) characteristic of bulk magnetite (*18*). With an increasingly severe reduction treatment the Mössbauer spectra show the presence of both Fe_3O_4 and α-Fe without any indication of an intermediate Fe^{2+} compound as with the Fe/Al_2O_3 catalyst.

Figure 8 shows a representative bright-field micrograph of the passivated Fe/Al_2O_3 catalyst (reduced 15 h at 873 K). The picture shows iron crystallites with a mean metal particle diameter between 20 and 30 nm. Prolonged reduction at this temperature does not markedly affect the particle size.

Fe/SiO_2 Catalyst

As with the alumina-supported iron catalyst no infrared-active adsorption occurred on the fresh, unreduced, and evacuated iron-on-silica catalyst.

Figure 9 shows the spectra recorded with an Fe/SiO_2 catalyst reduced under progressively more severe conditions. After high-temperature reduction the samples were evacuated at room temperature for 0.5 h. Subsequently, 13.3 kPa CO was dosed and spectra were recorded. After mild reduction a single band at 2170 cm^{-1} is present in the spectrum. Upon further reduction, apart from the band at 2170 cm^{-1} a small

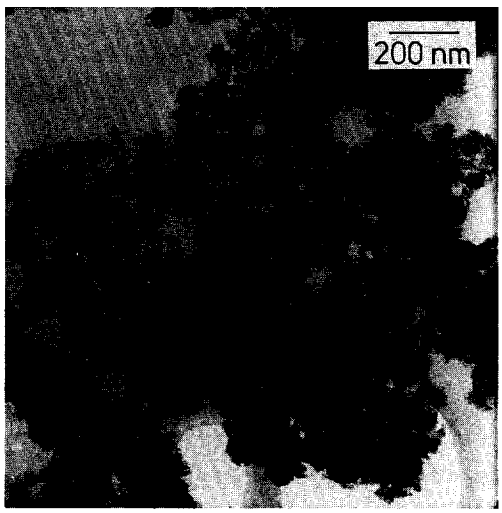

FIG. 8. Electron micrograph of reduced (15 h, 873 K) and passivated Fe/Al_2O_3 catalyst.

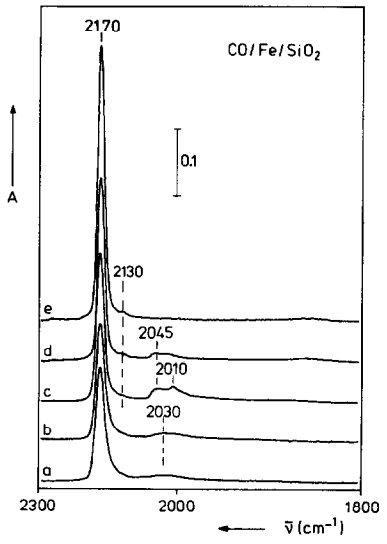

FIG. 9. Infrared spectra of adsorbed CO (13.3 kPa) on Fe/SiO_2 catalyst subsequently reduced under progressively more severe conditions: (a) 6 h, 623 K; (b) 15 h, 623 K; (c) 24 h, 723K; (d) 15 h, 873 K; (e) 2 h, 973 K.

band at 2130 cm^{-1} and a broad, weak band between 2010 and 2045 cm^{-1} appear in the spectrum. Upon reduction at a higher temperature, however, the 2010- to 2045-cm^{-1} band disappears, whereas the band at 2170 cm^{-1} remains present. The intensity of this band even increases with prolonged reduction time/temperature. Whereas the band at 2170 cm^{-1} is not stable against room temperature CO evacuation, the band at about 2010–2045 cm^{-1} is only slightly affected by evacuation.

Admission of 11 kPa O_2 for half an hour to the evacuated (partly) reduced catalyst completely suppressed adsorption of CO (not shown).

Especially the spectra shown in Figs. 9b and 9c change markedly upon prolonged room temperature CO exposure (shown in Fig. 10). It appears that upon prolonged CO exposure at room temperature the intensity of the 2170-cm^{-1} band decreases in favor of the intensity of the broad band around 2020 cm^{-1}. Furthermore, a new band simultaneously appears at 1620 cm^{-1}. In contrast to the band at 2170 cm^{-1}, both the 1620-cm^{-1} and the 2020-cm^{-1} bands are not appreciably affected by room temperature evacuation. Although less pronounced these changes were also observed with the catalyst reduced under more severe conditions.

The substantial differences between Fe/Al_2O_3 and Fe/SiO_2 catalysts displayed by

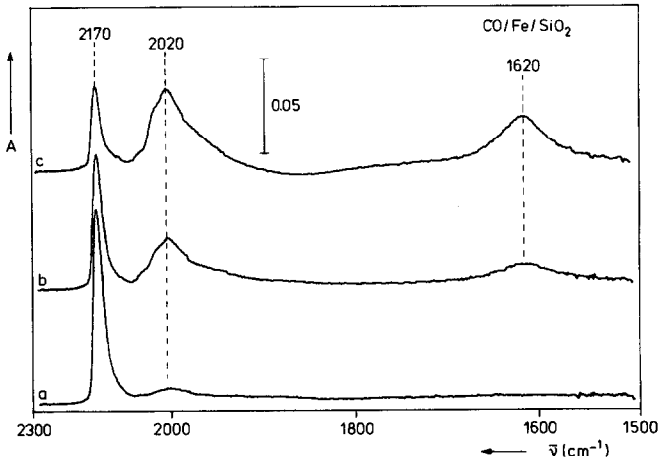

FIG. 10. Infrared spectra of adsorbed CO on reduced (24 h, 723 K) Fe/SiO_2 catalyst showing the effect of prolonged CO exposure (13.3 kPa) at room temperature. Spectra recorded after (a) 5 min, (b) 4 h, and (c) 23 h.

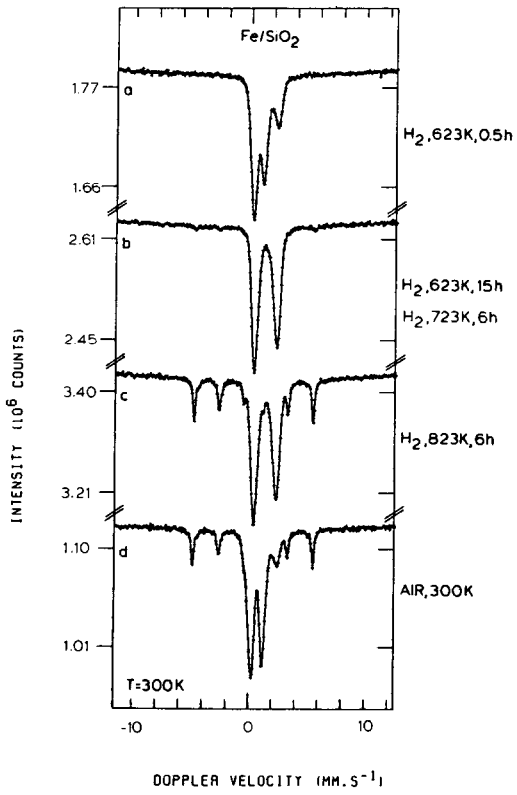

FIG. 11. Room temperature Mössbauer spectra of Fe/SiO_2 catalyst subsequently reduced under increasingly severe conditions.

infrared spectroscopy are also revealed by Mössbauer spectroscopy.

The Mössbauer spectra of the freshly prepared, unreduced iron-on-silica catalyst, measured at 300, 77, and 4.2 K, are shown in Fig. 5c. Since at 77 K only a doublet and at 4.2 K a markedly broadened sextuplet can be observed, the dispersion of the deposited α-FeOOH species is considerably higher than that of both the fresh, unreduced iron-on-alumina catalyst and the unreduced physical mixture of γ-Al_2O_3 and α-FeOOH (Figs. 5a and 5b, respectively).

The Mössbauer spectra recorded during the reduction of the Fe/SiO_2 are shown in Fig. 11. Careful reduction does not result in the formation of magnetite as with the Fe/Al_2O_3 catalyst. The spectrum shown in Fig. 11a, recorded after reduction at 623 K for 0.5 h, indicates the direct formation of an Fe^{2+} compound (IS = 1.22 mm/s and quadrupole splitting, QS = 2.30 mm/s). These Mössbauer parameters are essentially different from those of $Fe_{1-x}O$. The spectrum collected after prolonged high-temperature reduction (6 h, 823 K) shows the very slow formation of an α-Fe sextet. The predominant iron species present, however, is still an iron phase, which will be denoted "iron(II) silicate" for reasons to be discussed below. The intermediate iron(II) silicate phase prevents the formation of magnetite as well as that of a distinct $Fe_{1-x}O$ phase. Also the reduction to α-Fe is, compared to the physical mixture, considerably retarded. Exposure of the reduced catalyst to oxygen at room temperature converts the Fe^{2+} component almost completely to Fe^{3+}. This suggests that the iron(II) silicate formed is a surface compound. This assumption is supported by the appreciably broadened magnetically split pattern of this compound which is observed at 4.2 K (Fig. 12). The presence of α-Fe in the passivated catalyst shows that the dispersion of the iron particles is rather low. This is corroborated by electron micrographs of the Fe/SiO_2 catalyst reduced at 873 K for 16 h (Fig. 13b).

In Figs. 13a and 13b representative bright-field micrographs are shown of the Fe/SiO_2 samples reduced at 723 K for 150 h and at 873 K for 16 h. It can be seen in Fig. 13a that the mean particle size of the iron particles after reduction at 723 K is about 10 nm. It was established that the density of the iron particles increases only slowly upon prolonged reduction at 723 K, the particle size remaining essentially the same. Reduction during relatively short periods (16 h) at a higher temperature, however, leads to an appreciable increase of the mean particle size (d = 40–60 nm, Fig. 13b). It appears that relatively small iron particles are only formed after prolonged reduction at not too elevated temperatures.

In Fig. 14 the activity of the Fe/SiO_2 and Fe/Al_2O_3 catalysts in the Fischer–Tropsch

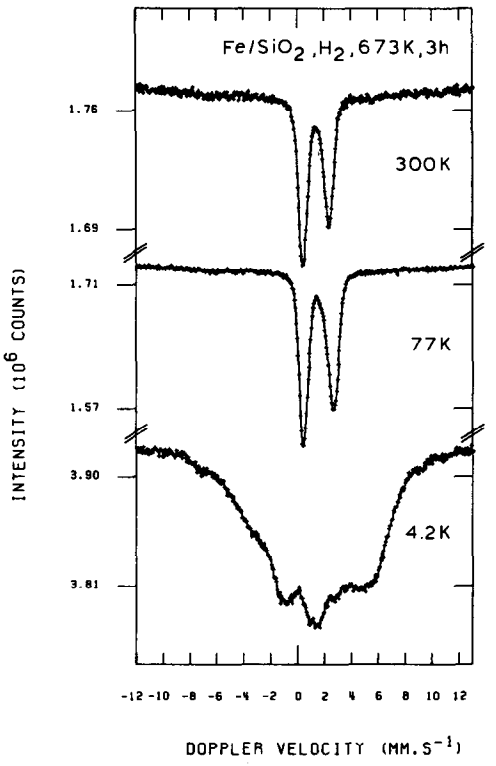

FIG. 12. Mössbauer spectra recorded at different temperatures of reduced (673 K, 3 h) Fe/SiO_2 catalyst.

synthesis is shown. Both catalysts have been reduced at 723 K for 16 h and before introduction of syngas they have been flushed with nitrogen for 1 h at 673 K. It can be seen that the activity (expressed per gram of iron) of the Fe/Al_2O_3 catalyst is about two orders of magnitude higher than that of the Fe/SiO_2 catalyst.

DISCUSSION

Reduction Behavior of the Catalyst

First, the Mössbauer spectra of the freshly prepared, unreduced catalysts will be discussed. As is shown in Table 1 the isomer shifts at 298 K appear to be the same for the two supported iron catalysts and the physical mixture of α-FeOOH and γ-Al_2O_3. Only the observed electric quadrupole splittings in the three cases are slightly different. Both Mössbauer parameters are characteristic of a high-spin Fe^{3+} species present in α-FeOOH (*16, 19, 20*). From the temperature dependence of the resonant absorption patterns an estimation of the dimensions of the α-FeOOH particles can be made. Van der Woude has investigated the temperature dependence of Mössbauer

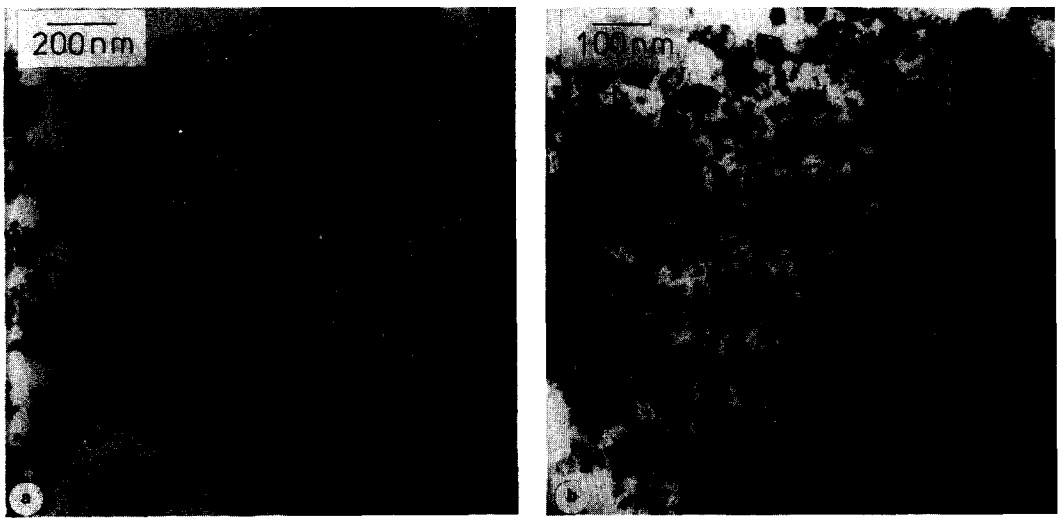

FIG. 13. Electron micrographs of reduced and passivated Fe/SiO_2 catalyst: (a) reduced for 150 h at 723 K and (b) reduced for 16 h at 873 K.

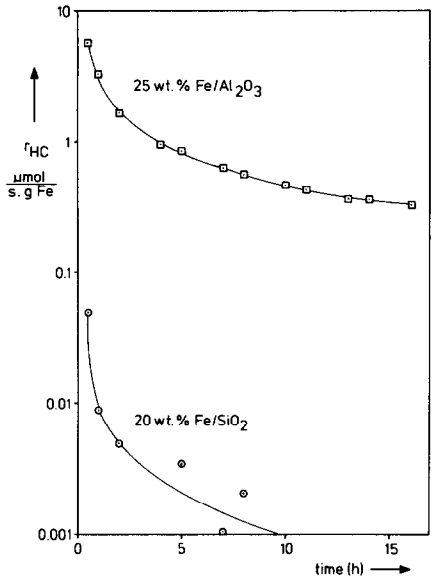

FIG. 14. The rate of CO conversion to hydrocarbons of the Fe/SiO_2 and Fe/Al_2O_3 catalysts.

spectra of goethite particles, the dimensions of which were estimated from electron micrographs (*17*). Using this calibration it follows from Fig. 5 that in the alumina-supported iron catalyst larger particles (8–10 nm) are present than in the silica-supported iron catalyst (2–3 nm). The particle size of the unsupported α-FeOOH sample is 4–8 nm. These results are corroborated by estimations based on XRD line broadening and BET surface area measurements (*3*). The quadrupole splittings of α-FeOOH have not been described in terms of separate doublets corresponding to contributions of surface atoms and core atoms, as has been reported for α-Fe_2O_3 (*21, 22*). Nevertheless, the observed increase of the mean electric quadrupole splitting with decreasing particle size supports such a core/shell model.

The Mössbauer spectra of the Fe/Al_2O_3 catalyst and those of the physical mixture of α-FeOOH and γ-Al_2O_3 show marked differences in the reduction behavior between these two samples. The first observation to be pointed out is that reduction of the physical mixture at 673 K for 0.5 h results in the formation of Fe_3O_4, which is characterized by bulk Mössbauer parameters and an insignificant line broadening. There was no indication of the presence of an intermediate iron oxide. On the other hand, the spectrum of the Fe/Al_2O_3 catalyst after reduction at 673 K exhibits a strongly broadened Fe_3O_4 component, an Fe^{2+} doublet (IS = 1.30 mm/s, QS = 0.55 mm/s), and part of the Fe^{3+} doublet associated with the starting material. The IS and the QS observed for the Fe^{2+} compound agree well with those reported for $Fe_{1-x}O$ (*23*). This compound is rather stable: the progress of the reduction to α-Fe with supported catalysts is considerably retarded compared to that of the physical mixture. The different extent of line broadening of the Fe_3O_4 compound in the alumina-supported catalyst and the physical mixture indicates that the dispersion of the Fe_3O_4 compounds is higher in the Fe/Al_2O_3 catalyst than in the physical mixture, whereas the reverse is true for the dispersion of the α-FeOOH particles originally present in the fresh, unreduced samples (vide supra). It should be recalled that substitution of foreign ions in the spinel iron oxide structure also causes some line broadening (*14, 15*).

Whereas commercial iron catalysts prepared by fusion of premixed Fe(II)/Fe(III) oxide and Al_2O_3 were found to reduce directly from the spinel to the metallic iron phase (*14, 24, 25*), *in situ* Mössbauer spectroscopy provides firm evidence that with alumina-supported catalysts the reduction to α-Fe proceeds consecutively via Fe_3O_4 (spinel) and $Fe_{1-x}O$ (NaCl structure).

We will now discuss the Mössbauer spectra collected during the reduction of the Fe/SiO_2 catalyst. The first striking observation is that during the reduction no magnetite (Fe_3O_4) is formed, which is in agreement with observations of Yuen *et al.* (*1*) studying the reduction behavior of a 1 wt% Fe/SiO_2 catalyst. Whereas our spectra show only one doublet due to Fe^{2+} cations, Yuen *et al.* observed during the reduction of the 1

wt% Fe/SiO_2 catalyst reduced at increasingly severe conditions two Fe^{2+} doublets. An inner doublet (IS = 1.06 mm/s; QS = 0.93 ± 0.03 mm/s) was attributed to cations of low coordination (denoted iron surface silicate by Yuen *et al.* (*1*)) and an outer doublet (IS = 1.28 mm/s; QS = 1.84 mm/s) was ascribed to Fe^{2+} cations of high coordination (present in highly dispersed iron(II) oxide particles). The presence of two doublets, the relative intensities of which varied with the reduction procedure, was observed by various other investigators studying the reduction behavior of Fe/SiO_2 catalysts (*1, 26–28*).

The Mössbauer parameters of the doublet in our Fe/SiO_2 catalyst (IS = 1.22 mm/s, QS = 2.30 mm/s) are very similar to the IS and QS of the outer doublet found in the above-mentioned studies (*1, 26–28*) suggesting (according to the interpretation given by Yuen *et al.*) that our doublet also arises from highly dispersed Fe^{2+} ions present in an iron(II) oxide phase. However, the observed QS of our doublet differs considerably from $Fe_{1-x}O$ (QS = 0.55 mm/s) (which was found with the Fe/Al_2O_3 catalyst), indicating that if this doublet indeed arises from Fe^{2+} cations in iron oxide particles, the structure of this oxide must be completely different from $Fe_{1-x}O$. In our view an intimate contact between the Fe^{2+} cations and the silica (i.e., reaction to iron(II) silicate) can more readily explain the observed features. In fact, the observed IS compares reasonably well with that of bulk Fe_2SiO_4 (IS = 1.41 mm/s (*29*)). The almost complete reoxidation of this compound by exposure to air at room temperature (Fig. 11d) indicates that this species is located at or near the surface, thereby explaining the lower QS compared to bulk Fe_2SiO_4 (QS = 2.81 mm/s). Furthermore, the spectra of bulk Fe_2SiO_4 show Zeeman splitting below 66 K (*29*). Figure 12 shows that a hyperfine pattern is only observed at 4.2 K supporting the above assignment; the broadening of the hyperfine pattern arises from the surface location. Bancroft *et al.* (*30*) have reported Mössbauer parameters for a number of iron(II) silicates with different crystal structures which are very similar to the Mössbauer parameters of the doublet of our study. We thus propose that the outer doublet found by Yuen *et al.* (*1*), Hobson and Gager (*26*) and Hobson and Campbell (*27*) should be ascribed to a compound which resembles iron(II) silicate rather than iron(II) oxide. This interpretation has also been proposed by Clausen (*28*).

Surface States of Supported Iron Particles

The Mössbauer results show that in the freshly prepared, unreduced iron-on-alumina and iron-on-silica catalysts iron is present as supported α-FeOOH. After room temperature evacuation no infrared active adsorption of carbon monoxide has been observed with these fresh catalysts. Furthermore, admission of CO to (partly) reduced and subsequently reoxidized catalysts gives only a small carbonate-like band at 1620 cm^{-1}. Since with both the fresh, unreduced samples and the reduced/reoxidized catalysts the valency of the iron cations is 3+, we conclude that on trivalent iron ions no infrared-active CO adsorption occurs which gives rise to absorption bands in the region around 2000 cm^{-1}.

Figure 1 shows that in the spectrum of the Fe/Al_2O_3 independently of the degree of reduction two intense bands are present, viz. a band at 2155 cm^{-1} and a low-frequency band consisting of two subbands at 2050 and 2010 cm^{-1}. Whereas the relative intensity of the latter two bands is strongly dependent on the severity of the reduction treatment (Fig. 1) and on the presence of carbon and/or oxygen in the surface (Fig. 3), it appears that the band at 2155 cm^{-1} is hardly affected by the applied reduction procedures. Deposition of carbon and/or oxygen leads to a band at 2085 cm^{-1}, which disappears upon treatment in CO at 573 K. Most probably the band at 2155 cm^{-1} arises from CO adsorbed on Fe^{2+} cations. Since

this band is present in the spectrum even after a prolonged reduction treatment (Fig. 2), it appears that these Fe^{2+} cations strongly interact with the support material (such as, e.g., surface iron aluminate) thus explaining the slow reduction. Since the band at 2085 cm^{-1} (Figs. 3b and 4b) only appears in the spectrum after reduction and subsequent deposition of carbon and/or oxygen layers, we propose that this band should be assigned to CO adsorbed on Fe^{2+} cations associated with oxygen and/or carbon present in the surface of the (partly) reduced iron particles. Since this band disappears upon a treatment with CO at 573 K (Fig. 3c), it follows that the oxygen associated with these particular iron cations is more easily removed than the oxygen associated with the iron cations giving rise to the 2155-cm^{-1} band. Although both the 2155-cm^{-1} band and the 2085-cm^{-1} band arise from adsorption onto Fe^{2+} cations, the vibration frequencies differ considerably. This can be understood since in the present interpretation the Fe^{2+} cations giving rise to the band at 2085 cm^{-1} are present in the surface of an iron particle the bulk of which is partly reduced, leading to an increased electron donating power of these Fe^{2+} ions compared to that of the Fe^{2+} ions present in the surface iron aluminate and thus explaining the lower vibration frequency.

The peak position of the 2050/2010-cm^{-1} band and the intensity increase with increasingly severe reduction treatment suggest that this band should be ascribed to CO adsorption on metallic iron atoms. According to Nguyen and Sheppard these vibration frequencies arise from linearly bonded CO molecules (*10*). The two different vibration frequencies at 2050 and 2010 cm^{-1} point to the presence of different reduced iron sites. Since on the oxygen- and/or carbon-covered surface the intensity of the 2050-cm^{-1} band increases at the expense of the intensity of the 2010-cm^{-1} band (Fig. 3b), the 2050-cm^{-1} band can be attributed to CO adsorbed on reduced iron atoms interacting with carbon and/or oxygen atoms and the 2010-cm^{-1} band to CO adsorbed on fully reduced, undisturbed iron atoms present in more extended iron facets. These assignments are in qualitative agreement with results of a recent HREELS study dealing with the adsorption of CO on clean and contaminated Fe(111) single crystal surfaces (*31*). Whereas on a clean Fe(111) surface a band due to linearly bonded CO molecules at 2000 cm^{-1} is observed, this band is centered around 2030 cm^{-1} on a surface precovered with small amounts of carbon and/or oxygen.

The presence of the 2155-cm^{-1} band and the subband at 2050 cm^{-1} in the spectra of the reduced Fe/Al_2O_3 catalyst indicate that the surfaces of the iron particles are not completely reduced.

Various explanations can be given for the absence of bridge-bonded CO adsorption in our experiments. If one assumes that the sites able to provide multiple coordination for CO molecules are blocked by the presence of oxygen (which is present in the surfaces of the reduced Fe/Al_2O_3 catalyst), it can be envisaged that even small residual amounts of oxygen are already sufficient to suppress bridge-bonded CO adsorption virtually completely: the probability of finding adjacent iron atoms capable of binding CO in a bridge-bonded configuration decreases more than proportionally with increasing oxygen levels. Furthermore, under our experimental conditions some dissociative adsorption of CO may occur (*32–36*) also leading to a suppression of bridge-bonded CO. Studying the adsorption of CO on an Fe(111) surface with HREELS Seip *et al.* (*31*) observed that dissociation of CO leads to a suppression of adsorption in the bridge-bonded configuration.

From Fig. 4 it follows that high-temperature evacuation after hydrogen reduction leads to appreciable changes in the spectrum of adsorbed CO: the intensity of the 2050/2010-cm^{-1} band decreases, whereas the intensity of the 2155-cm^{-1} band slightly increases and also the band at 2085 cm^{-1} appears in the spectrum. On the basis of the

above given assignments it appears that upon high-temperature evacuation considerable reoxidation of the partly reduced iron surface occurs. This can be explained by assuming that, in agreement with interpretations given by others (*5, 37, 38*), upon high-temperature evacuation water molecules are formed by hydrocondensation of hydroxyl groups from the support leading to reoxidation of the surface according to

$$Fe + H_2O \rightarrow \text{“}Fe^{2+}O\text{”} + H_2$$

Our results demonstrate that even after prolonged reduction treatments residual amounts of oxygen are present in the surface of the reduced Fe/Al_2O_3 catalyst. Recent results obtained with iron single crystal surfaces have shown that removal of the last monolayer of oxygen is a highly structure-sensitive process: full reduction of the more open Fe(100) surface is much more difficult than that of the close-packed Fe(110) surface (*39, 40*). These results suggest that full reduction of the surfaces of supported iron particles can only be brought about with relatively large iron (oxide) crystallites. Since the dimensions of the iron crystallites present in our reduced Fe/Al_2O_3 catalyst are between 20 and 30 nm (Fig. 8), it can be envisaged that full reduction of even smaller iron (oxide) particles becomes virtually impossible.

It is well known that with reduced iron catalyst containing small iron particles (<5 nm) the chemisorption of hydrogen at room temperature is suppressed at room temperature compared to the chemisorption of carbon monoxide (*6, 41–43*). Since with iron catalysts consisting of larger iron crystallites the hydrogen and carbon monoxide adsorption capacities are nearly equal, the activated hydrogen chemisorption at room temperature is characteristic for small iron particles suggesting that hydrogen chemisorption on iron surfaces is a structure-sensitive process (*6*).

Alternatively, however, it can be argued that residual amounts of oxygen present in the surfaces of the partly reduced iron crystallites explain the observed activated hydrogen chemisorption with small iron particles. Complete removal of the oxygen from the iron surface becomes more difficult with decreasing particle size. With regard to hydrogen chemisorption it is known that small amounts of oxygen drastically affect the kinetics of hydrogen chemisorption (*34*). With respect to carbon monoxide adsorption our results show that CO is readily adsorbed on a partly reduced iron catalyst. As a result it can be argued that residual amounts of oxygen may account for the low H_2/CO ratio observed with supported iron catalysts. Oxygen removal from iron surfaces, being a structure-sensitive process, may thus explain the suppressed hydrogen uptake observed for small iron crystallites. Furthermore, since the amount of oxygen present in the surfaces of the (partly) reduced iron particles strongly depends on the evacuation procedure applied, it thus appears that also the hydrogen chemisorption capacity is strongly influenced by the pretreatment procedure involved.

Compared to the alumina-supported iron catalyst the silica-supported iron catalyst exhibits quite different carbon monoxide adsorption features. Since the Mössbauer results have shown that upon reduction with the Fe/SiO_2 catalyst a substantial amount of iron(II) silicate is formed, the predominant presence of the band at 2170 cm^{-1} in the infrared spectra (Fig. 9) suggests that this band can be ascribed to CO adsorption on this iron(II) silicate species. The weak, broad band around 2010–2045 cm^{-1} is assigned to CO adsorbed on reduced iron atoms, and the weak band at 2130 cm^{-1} (Fig. 9) is most likely due to CO adsorption on Fe(II) ions present in the surfaces of the partly reduced particles. The band at 1620 cm^{-1} appearing in the spectra upon prolonged CO exposure (Fig. 10) is indicative of the formation of a carbonate-like species (*13*). An alternative assignment for such a low vibration frequency emerges from the HREELS results on iron single crystal surfaces. According

to Seip *et al.* (*31*) carbon monoxide adsorption into deep holes leads to a vibration frequency as low as 1530 cm^{-1}. As the surfaces of small metallic particles are relatively open the presence of such holes can be easily envisaged.

Mössbauer spectra show that reduction at temperatures above 623 K leads to the formation of metallic iron. Furthermore, electron micrographs of the Fe/SiO_2 sample reduced at 723 K show the presence of small iron particles. However, the infrared spectra of samples reduced above 623 K show only a very weak band at 2010–2045 cm^{-1} due to the adsorption on metallic iron atoms. Thus, although α-Fe is formed it is not present in the surfaces of the small iron particles suggesting that metallic iron is (partly) encapsulated by an iron(II) silicate layer which gives rise to CO adsorption at 2170 cm^{-1}. Prolonged exposure of the partly reduced Fe/SiO_2 catalyst to carbon monoxide has a rather remarkable result (Fig. 10): the intensity of the band around 2020 cm^{-1} (reduced iron atoms) increases at the expense of the intensity of the 2170-cm^{-1} band. This can be explained by assuming that the surfaces of the metallic iron particles are less easily accessible from the gas phase than the Fe(II) ions present in the iron(II) silicate compound. Furthermore, in order to offer an explanation for the intensity decrease of the 2170-cm^{-1} band, it seems that the iron particles change their shape upon CO adsorption and cover the surface of the support containing the Fe(II) ions. Alternatively, one may speculate that as a result of CO-induced iron segregation (which readily occurs with certain alloy catalysts (*45*)) the surfaces of the iron particles initially capped by the iron(II) silicate layer become enriched in reduced iron atoms.

The increase of the 2170-cm^{-1} band with increasing severity of reduction (Fig. 9) may be explained by assuming that although as a result of the reduction the total amount of iron(II) silicate decreases the dispersion of the remaining part increases, as has also been suggested by Yuen *et al.* (*1*).

With our Fe/SiO_2 catalyst the formation of the iron(II) silicate compound accounts for the slow reduction to the metallic state. Only prolonged reduction (150 h) at 723 K leads to the formation of small metallic iron particles of about 10 nm (Fig. 13a). It has been reported that reduction of iron(II) silicate to metallic iron requires a $p(H_2O)/p(H_2)$ ratio three orders of magnitude lower than that required for the reduction of Fe_2O_3 (*44*). At higher temperatures reduction of the iron(II) silicate compound can proceed at higher water vapor pressures and thus will occur more rapidly yielding, however, big sintered iron particles (Fig. 13b).

The processes that occur during the reduction of our Fe/SiO_2 catalyst are schematically shown in Fig. 15. It is interesting to note that although the iron loading of our catalyst is relatively high (20 wt%), the Fe(II) ions have completely reacted upon reduction at 623 K with the silica support to the typical iron(II) silicate compound. There is experimental evidence that formation of iron(II) silicate is only brought about when an intimate contact between the support and the iron precursor is achieved (*46, 47*). With the preparation procedures usually applied (such as, e.g., impregnation) exclusive formation of iron(II) silicate only takes place at low metal loadings. For instance, with a 10 wt% Fe/SiO_2 catalyst prepared via wet impregnation the CO absorption band at 2170 cm^{-1} (characteristic of CO adsorption on iron(II) silicate) has not been observed (*48*). Accordingly, various investigators have established that the reducibility of Fe/SiO_2 catalysts increases with the iron loading (*14, 15, 49*). Our results indicate that when the iron precursor (α-FeOOH) is present on the support in a highly dispersed state complete reaction of the Fe(II) ions to iron(II) silicate can be achieved even at higher metal loadings. The preparation procedure used in this work affords even at relatively high metal loadings

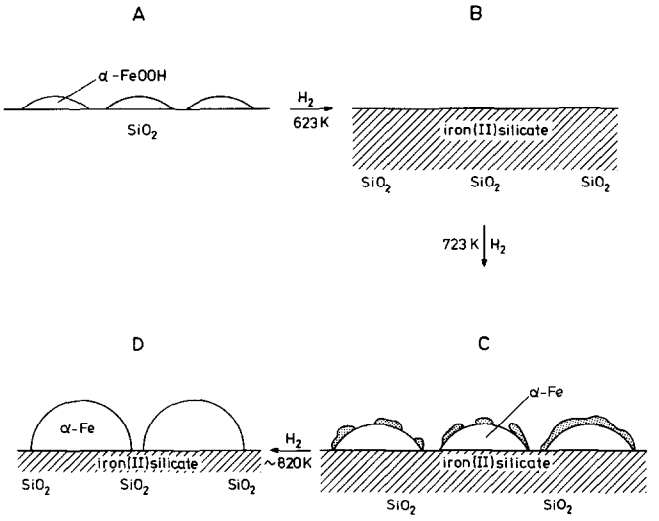

FIG. 15. Schematic representation of the reduction process of the Fe/SiO_2 catalyst.

the formation of highly dispersed α-FeOOH (2–3 nm) on the silica support. Finally, we mention that the formation of a metal silicate phase appears not to be exclusively restricted to Fe/SiO_2 catalysts. Using infrared spectroscopy and XPS Sato *et al.* (*50*) have observed the formation of cobalt(II) silicate during the reduction of a Co/SiO_2 catalyst.

Let us now address ourselves to the origin of the encapsulating layer present in the reduced Fe/SiO_2 catalyst. It is generally known that at elevated pressures and temperatures (e.g., 1.5 MPa at 500 K) water reacts with silica to give the volatile compound $Si(OH)_4$ (*51, 52*). Dumesic and Lund (*53*) have demonstrated, however, that silica in the presence of water becomes mobile at 670 K even at subatmospheric water pressure. Silica migration onto the iron surface during reduction may thus account for the formation of an encapsulating layer. However, separate experiments with a physical mixture of the Fe/Al_2O_3 catalyst and pure silica showed similar infrared absorption features to the pure Fe/Al_2O_3 catalyst.

A mechanism which could explain the formation of the encapsulation layer is based on the fact that during the reduction the iron precursor has completely reacted to iron(II) silicate. Recently, de Bokx *et al.* (*54*) have found evidence that the occurrence of the SMSI effect with Ni/TiO_2 is due to a transportation of titanium ions through the bulk of a nickel oxide particle, which proceeds by the intermediate formation of a nickel titanate ($NiTiO_3$) precursor. Upon reduction of this compound TiO_x species segregate to the surfaces of the thus formed nickel particles. In this mechanism bulk reduction proceeds, while the surface remains covered with inactive TiO_x species leading to the well-known characteristics of the SMSI effect. As the encapsulating layer found in our study is also formed after the iron(III) precursor has completely reacted to iron(II) silicate, the mechanism put forward by de Bokx *et al.* may account for our results as well.

Finally, the existence of an encapsulating layer has important consequences for the chemisorptive and catalytic properties of the iron-on-silica catalyst. Evidence is now provided to show why at least small silica-supported iron particles exhibit only a small extent of hydrogen chemisorption at room temperature. Furthermore, the results

readily explain the markedly lower Fischer–Tropsch activity of the silica-supported iron catalyst than of the alumina-supported sample.

CONCLUSIONS

Supported iron catalysts have been prepared by precipitating the iron precursors at constant pH onto a silica and an alumina support. The reduction behavior of these two catalysts has been investigated by means of Mössbauer and infrared spectroscopies. Our conclusions are as follows:

(i) Precipitation of an iron(III) precursor at constant pH into a suspension containing the support material leads to the deposition of highly dispersed supported α-FeOOH.

(ii) Both alumina- and silica-supported iron catalysts reduce via different intermediate Fe^{2+} compounds of considerable stability, which seriously retard reduction to α-Fe. The high temperature required to realize reduction to α-Fe brings about sintering of the metallic iron, especially in the case of the silica-supported catalyst. With the latter type of catalyst small supported iron particles are only obtained after prolonged reduction at not too high a temperature (723 K).

(iii) A detailed assignment of the various carbon monoxide vibration frequencies is presented. The infrared results show that full reduction of the surfaces of the alumina-supported iron crystallites is a slow process. Since results from single crystal surfaces have shown that removal of oxygen from iron surfaces is a highly structure-sensitive process, it is suggested that especially with small iron particles complete reduction of the surface is a slow process. Furthermore, it has been shown that high-temperature evacuation leads to a considerable reoxidation of the (partly) reduced iron surface.

(iv) The surfaces of the silica-supported iron particles are encapsulated by an iron(II) silicate layer. Upon prolonged CO exposure the amount of iron atoms exposed to the gas phase increases.

(v) Conclusions (iii) and (iv) may account for the usually observed activated hydrogen chemisorption with supported iron catalysts.

REFERENCES

1. Yuen, S., Chen, Y., Kubsh, J. E., Dumesic, J. A., Topsøe, N., and Topsøe, H., *J. Phys. Chem.* **86,** 3022 (1982).
2. Boudart, M., Delbouille, A., Dumesic, J. A., Khammouna, S., and Topsøe, H., *J. Catal.* **37,** 486 (1975).
3. Kock, A. J. H . M., Fortuin, H. F., and Geus, J. W., *J. Catal.* **96,** 261 (1985).
4. Niemantsverdriet, J. W., van der Kraan, A. M., Delgass, W. N., and Vannice, M. A., *J. Phys. Chem.* **89,** 67 (1985).
5. Dutartre, R., Bussière, P., Dalmon, J. A., and Martin, G. A., *J. Catla.* **59,** 59 (1979).
6. Topsøe, H., Topsøe, N., Bohlbro, H., and Dumesic, J. A., *in* "Proceedings, 7th International Congress on Catalysis, Tokyo, 1980" (T. Seiyama and K. Tanabe, Eds.), p. 247. Elsevier, Amsterdam, 1981.
7. Wielers, A. F. H., Aaftink, G. J. M., and Geus, J. W., *Appl. Surf. Sci.* **20,** 564 (1985).
8. Niemantsverdriet, J. W., Ph.D. thesis, University of Technology, Delft, The Netherlands, 1983.
9. De Bokx, P. K., Kock, A. J. H. M., Boellaard, E., Klop, W., and Geus, J. W., *J. Catal.* **96,** 454 (1985).
10. Sheppard, N., and Nguyen, T. T., *in* "Advances in Infrared and Raman Spectroscopy," Vol. 5. Heyden and Son, London, 1978.
11. Toolenaar, F. J. C. M., Ph.D. thesis, University of Leiden, The Netherlands, 1983.
12. Körner, H., Landes, H., Wedler, G., and Kreuzer, H. J., *Appl. Surf. Sci.* **18,** 361 (1984).
13. Hair, M. L., *in* "Infrared Spectroscopy in Surface Chemistry." Dekker, New York, 1967.
14. Topsøe, H., Dumesic, J.. A., Mørup, S., *in* "Applications of Mössbauer Spectroscopy" (R. L. Cohen, Ed.), Vol. 2, p. 55, Academic Press, New York.
15. Dumesic, J. A., and Topsøe, H., *Adv. Catal.* **26,** 121 (1977).
16. Forsyth, J. B., Hedley, I. G., and Johnson, C. E., *J. Phys. C* **1,** 179 (1968).
17. Van der Woude, J. H. A., Ph.D. thesis, University of Utrecht, The Netherlands, 1983.
18. "Mineral Data Handbook" (J. G. Stevens, H. Pollak, L. Zhe, V. E. Stevens, R. M. White, and J. L. Gibson, Eds.). Mössbauer Effect Data Center, Asheville, North Carolina, 1983.
19. Gager, H. M., and Hobson, M. C., *Catal. Rev. Sci. Eng.* **11,** 117 (1975).
20. Golden, D. C., Bowen, L. H., Weed, S. B., and J. Bigham, J., *Soil Sci. Amer. J.* **43,** 802 (1979).

21. Kündig, W., Ando, K. J., Lindquist, R. H., and Constabaris, G., *Czech. J. Phys. B* **17,** 467 (1967).
22. Van der Kraan, A. M., *Phys. Status Solidi A* **18,** 215 (1973).
23. Greenwood, N. N., *in* "Proceedings, Int. Conf. Appl. Mössbauer Effect, 1972" (S. G. Cohen and M. Pasternak, Eds.), p. 30. Plenum, New York, 1973.
24. Ludwiczek, H., Preisinger, A., Fisher, A., Hosemann, R., Schönfeld, A., and Vogel, W., *J. Catal.* **51,** 326 (1978).
25. Clausen, B. S., Mørup, S., Topsøe, H., Candia, R., Jensen, E. I., Baranski, A., and Pattek, A., *J. Phys. Colloq.* **37,** C6-245 (1976).
26. Hobson, M. C., and Gager, H. M., *J. Colloid Interface Sci.* **34,** 357 (1970).
27. Hobson, M. C., and Campbell, A. D., *J. Catal.* **8,** 294 (1967).
28. Clausen, B. S., Ph.D. thesis, Technical University of Denmark, Lyngby, 1979.
29. Kündig, W., Cape, J. A., Lindquist, R. H., and Constabaris, G., *J. Appl. Phys.* **38,** 947 (1967).
30. Bancroft, G. M., Maddock, A. G., and Burns, R. G., *Geochim. Cosmochim. Acta* **31,** 2219 (1967).
31. Seip, U., Tsai, M.-C., Christmann, K., Küppers, J., and Ertl, G., *Surf. Sci.* **139,** 29 (1984).
32. Wedler, G., and Ruhmann, R., *Appl. Surf. Sci.* **14,** 137 (1982).
33. Broden, G., Gafner, G., and Bonzel, H. P., **13,** 33 (1977); *Surf. Sci.* **84,** 295 (1979).
34. Benziger, J., and Madix, R. J., *Surf. Sci.* **94,** 119 (1980).
35. Vink, T. J., Gijzeman, O. L. J., and Geus, J. W., *Surf. Sci.* **150,** 14 (1985).
36. Textor, M., Gay, I. D., and Mason, R., *Proc. R. Soc. London A* **356,** 37 (1977).
37. Perrichon, V., Primet, M., Nahon, M., and Turlier, P., *C.R. Acad. Sci. Ser. 2* **89,** C-149 (1979).
38. Nahon, N., Perrichon, V., Turlier, P., and Bussière, P., *React. Kinet. Catal. Lett.* **11,** 281 (1979).
39. Vink, T. J., der Kinderen, J. M., Gijzeman, O. L. J., and Geus, J. W., *Appl. Surf. Sci.* **26,** 367 (1986); Vink, T. J., Sas, S. J. M., Gijzeman, O. L. J. and Geus, J. W., *J. Vac. Sci. Technol. A* **5,** 1028 (1987).
40. Kock, A. J. H. M., and Geus, J. W., *Prog. Surf. Sci.* **20,** 165 (1985).
41. Rodriguez-Reinoso, F., de Dios Lopez-Gonzales, J., Moreno-Castilla, C., and Rodrigues-Ramos, I., *Fuel* **63,** 1089 (1984).
42. Vannice, M. A., Walker, P. L., Jung, H.-J., Moreno-Castilla, C., and Mahajan, O. P., *in* "Proceedings, 7th International Congress on Catalysis, Tokyo, 1980" (T. Seiyama and K. Tanabe, Eds.), p. 245. Kodansha/Elsevier, Tokyo/Amsterdam, 1981.
43. Jung, H.-J., Vannice, M. A., Mulay, L. N., Stanfield, R. M., and Delgass, W. N., *J. Catal.* **76,** 208 (1982).
44. Bouwman, R., Lippens, G. J. M., and Sachtler, W. M. H., *J. Catal.* **25,** 350 (1972) (Pd/Ag); Verbeek, H., and Sachtler, W. M. H., *J. Catal.* **42,** 257 (1976) (Pt/Sn); Van Dijk, W. L., Groenewegen, J. A., and Ponec, V., *J. Catal.* **45,** 277 (1976) (Ni,Cu).
45. Huang, Y. Y., and Anderson, J. R., *J. Catal.* **40,** 143 (1975).
46. Bianchi, D., Batis-Landoulsi, H., Bennett, C. O., Pajonk, G. M., Vergnon, P., and Teichner, S. J., *Bull. Soc. Chim. Fr.* **9–10,** I-345 (1981).
47. Heal, M. J., Leisegang, E. C., and Torrington, R. G., *J. Catal.* **51,** 314 (1978).
48. Blyholder, G., and Neff, L. D., *J. Phys. Chem.* **66,** 1464 (1962).
49. Guczi, L., *Catal. Rev. Sci. Eng.* **23,** 329 (1981).
50. Sato, K., Inoue, Y., Kojima, I., Miyazaki, E., and Yasumori, I., *J. Chem. Soc. Faraday Trans 1* **80,** 841 (1984).
51. Prigogine, M., and Fripiat, J. J., *J. Chem. Phys. Lett.* **12,** 107 (1971).
52. Everett, D. H., Haynes, J. M., and McEllroy, P., *Nature (London)* **226,** 1033 (1970).
53. Lund, C. R. F., and Dumesic, J. A., *J. Catal.* **72,** 21 (1981).
54. De Bokx, P. K., Bonne, R. L. C., and Geus, J. W., *Appl. Catal.* **30,** 33 (1987).